X-ray photoemission from small mercury clusters on II-VI semiconductor surfaces

R. Sporken,* S. Sivananthan, J. Reno,† and J. P. Faurie
Department of Physics, University of Illinois at Chicago, P.O. Box 4348, Chicago, Illinois 60680
(Received 16 October 1987)

The presence of small Hg clusters ($R = 5-20$ Å) on $Hg_{1-x}Cd_xTe$ samples grown by molecular-beam epitaxy has been deduced from a careful analysis of the x-ray-induced photoemission spectra. The positive binding-energy shift measured for these clusters is explained by the appearance of a positive charge on the clusters during the photoemission process. (The experimental results are compared with the calculated $e^2/2R$ behavior.) The apparent spin-orbit splitting for the Hg $5d$ levels is reduced, compared to bulk Hg and to isolated Hg atoms. This is attributed to the repulsion between the Cd $4d$ and Hg $5d$ orbitals. It is shown that Hg out-diffusion is the main reason for the formation of these clusters.

I. INTRODUCTION

Studies of surfaces and interfaces of semiconducting materials are very important for the development and understanding of modern microelectronic devices. Detailed investigation of the phenomena occurring during the growth of such surfaces and interfaces is very important due to the still increasing miniaturization of the devices presenting a challenge to both theoreticians and experimentalists. This paper deals with one particular aspect of surface studies on II-VI compound semiconductors, which is the formation of small mercury clusters on the surfaces of these semiconductors.

Photoemission has been demonstrated to be very powerful for examining the electronic properties of supported small metal clusters.[1-3] The study of such small particles was initially motivated by their technological importance in heterogeneous catalysis.[4] Small metal clusters have also been detected in many cases during the early stages of metal-semiconductor interface formation.[5-7] Amorphous carbon has been the most widely used substrate for detailed studies of the electronic properties of small metal clusters, but other substrates, mostly insulators, have been used as well. In this paper we present a photoemission study of Hg clusters on CdTe(111) and $Hg_{1-x}Cd_xTe(111)$ substrates. To the best of our knowledge, this is the first detailed photoemission study of metal clusters on a semiconducting substrate.

This work was first motivated by an unexpected result obtained during the study of the Hg incorporation in CdTe during the growth of HgTe-CdTe superlattices by molecular-beam epitaxy (MBE).[8] The common growth technique for HgTe-CdTe superlattices and other superstructures, such as single and double barrier tunneling structures, involves leaving the Hg cell open at all times.[9,10] As a result, the CdTe layers are not pure CdTe layers, but instead $Hg_{1-x}Cd_xTe$ with typically 3–9 % of mercury for the (111) B orientation.[8] In addition to Hg bound to Te atoms, the x-ray photoemission (XPS) analysis of such spectra revealed the existence of a second type of mercury with about 600 meV higher binding energy.[8] In the present work, we show that this second mercury component in the Hg $5d$ and $4f$ spectra is due to the presence of small Hg clusters on CdTe and $Hg_{1-x}Cd_xTe$ surfaces. The electronic properties as well as the origin of these clusters will be discussed.

II. EXPERIMENT

The samples were all prepared at the University of Illinois at Chicago in a Riber MBE 2300 machine. CdTe substrates oriented in the (111) B direction as well as GaAs substrates with a CdTe(111) B buffer layer were used. The substrate preparation and the growth of the appropriate buffer layer have been discussed elsewhere.[9] The layers analyzed here are $Hg_{1-x}Cd_xTe$ with x in the range of 0.15–0.97. The smaller x values were obtained with three MBE sources (CdTe, Te, and Hg) following the usual procedure.[9] The larger values are obtained with only two sources (CdTe and Hg) as described in Ref. 8. The sample temperatures quoted here were measured using a Chromel-Alumel thermocouple and—whenever possible—by an infrared pyrometer. These measurements have been calibrated using the melting points of indium and tin.

The samples were kept under ultrahigh-vacuum conditions as they were transferred to the XPS chamber. The XPS measurements were performed with a SSX-100 spectrometer from Surface Science Laboratories. A monochromatized and focussed Al $K\alpha$ excitation line was used. The overall energy resolution measured on the Au $4f$ core level is 0.7 eV. The reference levels used for this study will be specified as necessary. The position of the Fermi level was determined from the position of the Au $4f_{7/2}$ line measured from a bulk gold sample. The corresponding binding energy was fixed at 83.93 eV. The core levels used in this work are the Hg $4f$ and $5d$, the Cd $3d$ and $4d$, and the Te $4d$ and $3d$. For all the peaks, the values of the area, position, and full width at half maximum (FWHM) were determined by a least-squares fit of individual spin-orbit doublets to the data.

III. RESULTS AND DISCUSSION

The discussion of the results will be organized in three parts. First, we will focus on a detailed analysis of the XPS spectra from $Hg_{1-x}Cd_xTe$ samples. It will be shown that two types of Hg exist in these samples, one being Hg bound to Te and the other due to the presence of small mercury clusters on the sample surface. Thereafter, it will be shown that such Hg clusters can be obtained by depositing Hg on CdTe(111) *B* surfaces at room temperature. Finally, we will try to identify the origin of these clusters obtained unintentionally on MBE-grown $Hg_{1-x}Cd_xTe$ surfaces.

Typical photoemission spectra from $Hg_{1-x}Cd_xTe$ are shown in Fig. 1. The peaks are the Cd 4*d* and Hg 5*d* spin-orbit doublets and the Hg $4f_{7/2}$. These spectra have been analyzed for all the samples by means of a least-squares curve-fitting procedure as mentioned above. A nonlinear background was subtracted from the spectra prior to the fitting procedure. The line shape used for the fits was a Lorentzian convoluted with a Gaussian. This procedure is justified for the photoemission from semiconductors. It might be argued, however, that the Doniach-Šunjić line shape[11] has to be used in the case of small metal clusters. The quality of the fits obtained with the symmetric line shape is very good. This might indicate that the final-state screening in very small clusters is different from bulk metals, resulting in a different (and smaller) singularly index for the Doniach-Šunjić line shape for these clusters as compared to the bulk metal.

Two types of Hg have consistently been found for all the samples. These two types of mercury will be labeled $Hg^{(1)}$ and $Hg^{(2)}$ in the following discussion. From its binding energy with respect to the valence-band maximum (VBM),[12] $Hg^{(1)}$ is clearly identified as Hg in $Hg_{1-x}Cd_xTe$. The second component $Hg^{(2)}$ is observed at higher binding energy. We have suggested earlier that $Hg^{(2)}$ is due to some kind of surface mercury.[8] This was inferred from two observations. First, on a 1.5-μm-thick CdTe layer grown with a Hg flux, the amount of incorporated Hg as measured with energy-dispersive x-ray spectroscopy (EDS) agrees with the results from XPS obtained by neglecting $Hg^{(2)}$. Including $Hg^{(2)}$ yields significantly higher concentrations. As the depth probed by XPS is small compared to EDS, $Hg^{(2)}$ should be located in the surface region. Second, the Hg concentration in the CdTe layers can be determined from the binding energy of the Cd 4*d* and Hg 5*d* levels with respect to the VBM. This procedure is described in Ref. 8. Once again these results agree with concentrations deduced from XPS peak areas, neglecting $Hg^{(2)}$. This also suggests that $Hg^{(2)}$ is located at the surface. Otherwise it would affect the position of the VBM.

Now that we have established that $Hg^{(2)}$ is some sort of surface mercury, we need to find its exact nature. From the chemical shift measured on the Hg 5*d* and Hg 4*f* lines, $Hg^{(2)}$ could be tentatively identified as $HgTe_2$. This is not a stable compound, but could exist at the surface of $Hg_{2-x}Cd_xTe$ samples. However, if $Hg^{(2)}$ is located in a two-dimensional surface layer, coverages up to 0.8 monolayers (ML) are deduced from the $Hg^{(2)}$ peak areas. Such a coverage should then affect the characteristics of a surface component detected in the Te 4*d* spectra. The surfaces studied here are (111) *B* surfaces which are ter-

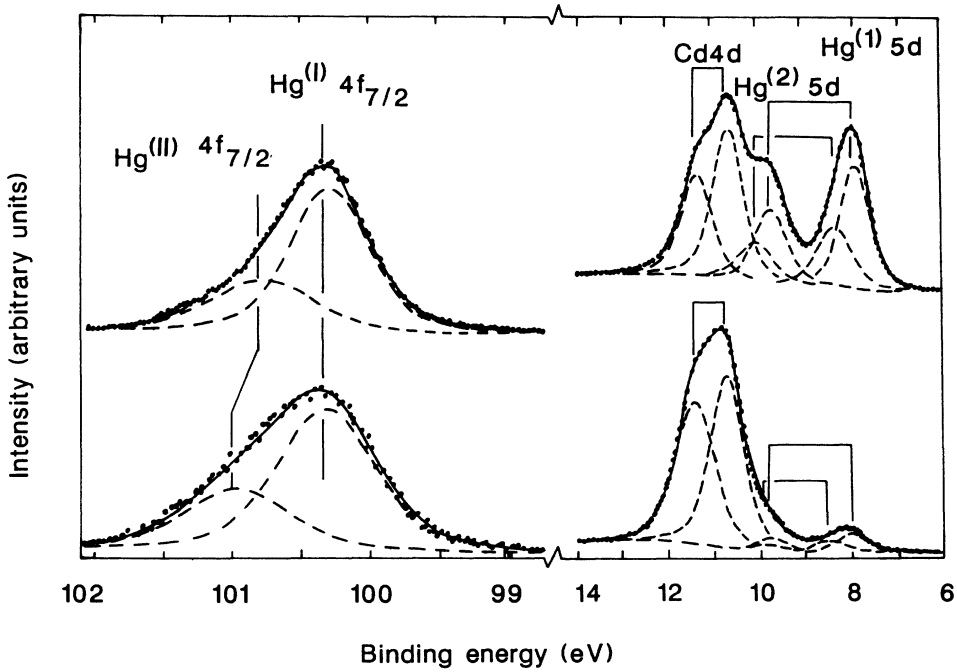

FIG. 1. Typical XPS core-level spectra from $Hg_{1-x}Cd_xTe$. The composition is $x=0.94$ (lower spectrum) and $x=0.60$ (upper spectrum). The number of atoms in the $Hg^{(2)}$ estimated using relation (1) is 7×10^{13} and 6×10^{14} cm^{-2}, respectively. The binding energy is referred to the Fermi level. The solid line is obtained by least-squares fitting of individual components (dashed lines) to the data.

minated by threefold-bonded Te atoms. From the Te 4*d* core-level spectra, a surface shift[13] of 475±75 meV towards higher binding energy was unambiguously determined by very careful curve fitting (Fig. 2). Close examination of the residuals, i.e., the difference between the calculated and the measured spectra, was particularly useful for the determination of this surface component. The characteristics (relative intensity, FWHM, and shift) of this surface component are independent of the amount of $Hg^{(2)}$. This rules out the existence of a two-dimensional layer of $HgTe_2$.

Based on this observation and on the fact that the Te 4*d* core-level intensity is reduced by only 5% for a $Hg^{(2)}$ coverage corresponding to 1 ML in the case of a two-dimensional layer, we suggest that $Hg^{(2)}$ must be related to the existence of small Hg clusters on the sample surface. The spectral characteristics of such small metal clusters are now well established[1-3,14,15] although the detailed explanation of these same characteristics is still a matter of debate. For almost all cases of small metal clusters, the core-level binding energies are higher than for the corresponding bulk material. This binding energy generally decreases with increasing cluster size, and sometimes a saturation or even a slight decrease is observed for very small cluster sizes.[3,14]

Figure 3 shows the binding energy E_B with respect to the Fermi level for the $Hg^{(2)}$ $4f_{7/2}$ core level versus the $A(Hg^{(2)}\,4f_{7/2})/A(\text{Te}\,3d_{5/2})$ area ratio. These data have been measured from many different samples and the different area ratios are the results of different preparation conditions. The relation between this area ratio and the preparation conditions will be discussed in the last section of this paper. The $A(\text{Hg})/A(\text{Te})$ area ratio is related to the average cluster radius. The intensity model described in Ref. 14 can be adapted to the present problem and the following relation is obtained:

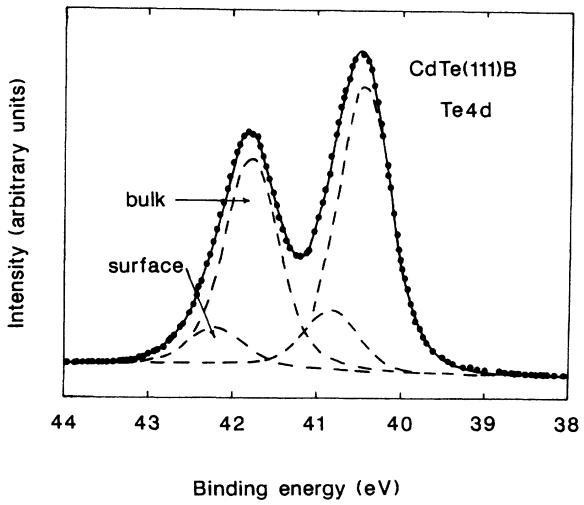

FIG. 2. Te 4*d* core-level spectrum from CdTe(111) *B*. The solid line is obtained by least-squares fitting of individual components (dashed lines) to the data. The binding-energy scale is referred to the Fermi level.

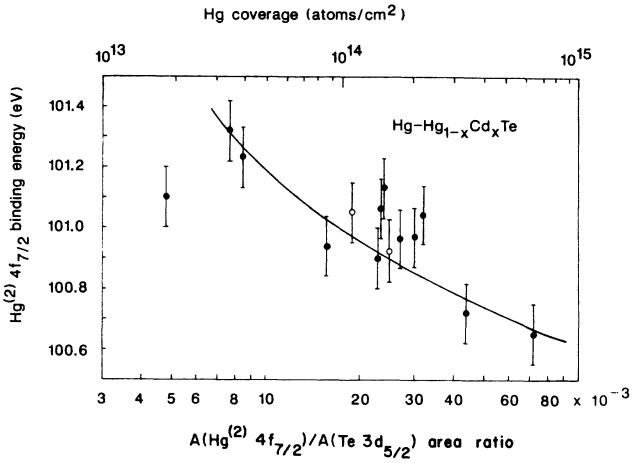

FIG. 3. $Hg^{(2)}$ $4f_{7/2}$ binding energy with respect to the Fermi level vs $A(Hg^{(2)}\,4f_{7/2})/A(\text{Te}\,3d_{5/2})$ area ratio. The solid circles are results from $Hg_{1-x}Cd_xTe$ samples, whereas the open circles are obtained after the Hg absorption on CdTe at room temperature. The Hg coverage has been estimated using relation (1) with $N_c=6\times10^{11}$ cm^{-2}. The solid line represents the calculated $e^2/2R$ behavior. For details see the text.

$$\Gamma = A(Hg^{(2)}\,4f_{7/2})/A(\text{Te}\,3d_{5/2})$$
$$= N_c k\lambda_e\{R^2-2[\lambda_e^2-(R\lambda_e+\lambda_e^2)\exp(-R/\lambda_e)]\}\ . \quad (1)$$

This relation is valid as long as the area covered by the clusters is small compared to the total sample area. R is the average cluster radius, N_c the cluster concentration, λ_e the effective photoelectron escape depth, and k is a constant depending on XPS sensitivity factors and on the density of the Hg clusters. λ_e is related to the photoelectron escape depth λ and to the mean electron escape angle β ($\lambda_e=\lambda\cos\beta$). If N_c has approximately the same value for all the samples studied here, a plot of E_B versus Γ is equivalent to a plot of E_B versus R on a nonlinear scale. Some scatter observed from our data is most likely due to slight differences in N_c between different samples. The binding-energy decrease observed in Fig. 3 with increasing cluster size is a common feature for small metal clusters. In the case of metal clusters supported on insulating substrates, Wertheim *et al.*[3,15] have shown that positive binding-energy shifts with decreasing cluster size can be attributed to the Coulomb energy $\sim e^2/2R$ which is due to the positive charge appearing on the cluster surface during the photoemission process. The unit charge in the photoemission final state is not neutralized during the time scale relevant to photoemission. The resulting Coulomb attraction will therefore increase the measured binding energy of the photoelectrons from the cluster. The same explanation was used in Ref. 14 for the case of Al clusters on Sb(111) substrates. We now suggest that this explanation may also be extended to the case of small metal clusters on certain semiconducting surfaces. For a typical cluster concentration of $N_c=6\times10^{11}$ cm^{-2}, the cluster radii corresponding to Fig. 3 are found in the range of 5–20 Å using Eq. (1). A rough estimation of the

corresponding $Hg^{(2)}$ coverages Θ yields $10^{13}-10^{15}$ atoms/cm^2. These coverage values are rather insensitive to the values of N_c, whereas the quoted radii are more strongly dependent on N_c. The reasonably smooth behavior of the data in Fig. 3 over a narrow range for the cluster radii (5–20 Å) is an indirect evidence for N_c being relatively independent on the details of the sample preparation. Figure 3 compares very well with results published in the recent literature concerning Au on amorphous carbon[2,3] and Ag on amorphous carbon.[15] In all the cases, the binding energy for the bulk metal was obtained for coverages between 10^{15} and 10^{16} atoms/cm^2. Extrapolation of our results, according to a $e^2/2R$ dependence, yields $E_B(Hg^{(2)}\ 4f_{7/2})=100.2\pm0.2$ eV for large cluster sizes. This is close to the value for bulk Hg (99.9 eV).[16] The solid line in Fig. 3 shows this $e^2/2R$ behavior adjusted to our data, using the values for R deduced from Eq. (1) with $N_c=6\times10^{11}$ cm^{-2}. There might be a saturation or even a slight decrease for very small cluster sizes, as already reported for Al on Sb(111).[14] However, we do not want to draw this conclusion, due to the insufficient number of data in this particular region.

Another striking feature of $Hg^{(2)}$ is the variation of the apparent spin-orbit splitting of the $Hg^{(2)}$ $5d$ levels with $Hg^{(2)}$ coverage Θ. Figure 4 shows this energy separation versus the intensity ratio Γ defined above. A total increase of 0.5 eV is observed with increasing cluster size. A saturation occurs at 1.7 eV, which is close to the value for bulk Hg (1.86 eV).[17] The spin-orbit splitting for isolated Hg atoms is known to be equal to the value for liquid Hg.[17] Our measured values of the apparent spin-orbit splitting are thus even smaller than the value for isolated atoms. This can be explained by the repulsion between the Cd $4d$ and Hg $5d$ levels, as initially discussed by Moruzzi *et al.*[18] In systems with two d metals, even with no direct energy overlap, the two sets of d levels interact. The result is a repulsion between these d states proportional to their original energy separation, which then reduces the apparent spin-orbit splitting of either subsystem. For the smallest clusters, almost all the $Hg^{(2)}$ atoms are in contact with the $Hg_{1-x}Cd_xTe$ surface, whereas the repulsion is reduced for the larger clusters due to the increased Cd—$Hg^{(2)}$ distance. A similar explanation has been invoked by Eberhardt *et al.* in the case of Cu_3Au alloys.[19]

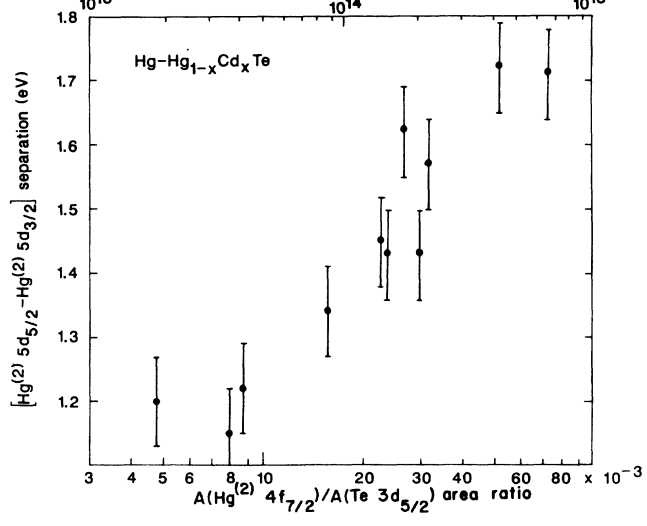

FIG. 4. $Hg^{(2)}$ $5d$ apparent spin-orbit splitting vs $A(Hg^{(2)}\ 5f_{7/2})/A(\text{Te}\ 3d_{5/2})$ area ratio. The Hg coverage has been estimated using relation (1) with $N_c=10^{11}$ cm^{-2}. For details see the text.

We have adsorbed Hg on MBE-grown CdTe(111) samples. The samples were kept at room temperature and the estimated Hg flux was approximately 2.5×10^{17} atoms cm^{-2} s^{-1}. This value was determined using Knudsen's effusion law. Hg $4f$, Cd $3d$, and Te $3d$ spectra have been measured after exposures of 35 and 45 min, respectively. Only one component was then detected in the Hg $4f_{7/2}$ spectra. The corresponding results are represented by the open circles in Fig. 3. These results agree with values measured for $Hg^{(2)}$ on $Hg_{1-x}Cd_xTe$. This is a further evidence that our interpretation of $Hg^{(2)}$ is correct. We also note that for these two exposures, the ratio of the Hg coverages quoted in Fig. 3 is in excellent agreement with the ratio of the Hg exposures.

The last section of this paper is devoted to a tentative identification of the origin of the Hg clusters on $Hg_{1-x}Cd_xTe$ surfaces. Two possible sources of these Hg clusters are readily identified: either the Hg in the $Hg_{1-x}Cd_xTe$ crystals or the residual Hg in the growth chamber during the cooling of the grown layers.

The cooling of the layers from the growth temperature (175–195 °C) to a temperature low enough to take the samples out of the growth chamber (typically 50 °C) takes on the order of 1 h. During this time, the Hg flux is progressively reduced from a value of typically 1.5×10^{17} atoms cm^{-2} s^{-1} to zero. The amount of Hg in the clusters obtained by this procedure is comparable with the amount obtained by exposing a CdTe(111) B surface at room temperature to an estimated Hg flux of 2.5×10^{17} atoms cm^{-2} s^{-1} during at least 30 min. As the Hg sticking coefficient on CdTe is expected to decrease with increasing temperature and based on the fact that the Hg flux used for the adsorption experiment was always higher than during the cooling of the $Hg_{1-x}Cd_xTe$ samples, we conclude that Hg adsorption on the $Hg_{1-x}Cd_xTe$ surfaces during the cooling cannot be the only reason for the formation of Hg clusters on these surfaces. We therefore suggest that out-diffusion of Hg from the samples contributes significantly to the formation of the Hg clusters.

A mercury atom reaching the surface of a $Hg_{1-x}Cd_xTe$ sample can (1) combine with any available free Te atom, (2) migrate on the surface until it reaches a nucleation site and contribute to the formation of Hg clusters, or (3) desorb from the surface. Parameters like the substrate temperature or the number and type of surface defects certainly play a major role in determining which of these steps will be the dominant one. The three possibilities exist regardless of whether the Hg atom reaches the surface by out-diffusion from the bulk or by condensation from the Hg vapor. However, it is clear

that the amount of Hg in the sample should affect the amount of Hg in the clusters if out-diffusion is the major source of Hg atoms going into the clusters. Such a relation has been observed (Table I). For different samples prepared at the same temperature, the amount of Hg in the clusters is found to increase with the Hg concentration in the $Hg_{1-x}Cd_xTe$ samples. The exact relationship between the two intensities certainly depends on the distribution of the Hg in the clusters and in the $Hg_{1-x}Cd_xTe$, as well as on the details of the diffusion mechanism. Furthermore, the data in Table I are consistent with the assumption that the amount of Hg in the clusters increases with increasing temperature for a given sample composition. This would not be easy to explain if condensation from Hg vapor was the main reason for the cluster formation, whereas enhanced out-diffusion combined with higher surface mobility is likely to increase the amount of Hg in the clusters. However, increasing the substrate temperature also favors the Hg desorption. Many more experimental results as well as a detailed study of the corresponding surface kinetics are thus called for. A future study should also reveal whether the out-diffusing Hg was initially bound to Te or instead located in interstitial lattice sites. This is very important for an understanding of the thermal stability of these materials. The existence of interstitial Hg is indeed expected due to the high Hg overpressure needed during the growth of $Hg_{1-x}Cd_xTe$.[20]

TABLE I. Intensity ratio $A(Hg^{(2)}\ 4f_{7/2})/A(Te\ 3d_{5/2})$ for the Hg clusters along with the growth temperature and the composition of the $Hg_{1-x}Cd_xTe$ samples.

T_s (°C)	$1-x$	$A(Hg^{(2)}\ 4f_{7/2})/A(Te\ 3d_{5/2})$
185	0.065	9.7×10^{-3}
185	0.740	4.4×10^{-2}
195	0.045	4.8×10^{-3}
195	0.057	9.3×10^{-3}
195	0.085	1.6×10^{-2}
175	0.095	7.7×10^{-3}
185	0.065	9.7×10^{-3}
195	0.057	9.3×10^{-3}

IV. CONCLUSION

We have shown that Hg clusters are found on MBE-grown $Hg_{1-x}Cd_xTe$ samples. The typical radius of these clusters is in the range of 5–20 Å. The Hg core levels measured with XPS show the typical positive binding-energy shift which increases with decreasing cluster size. This shift is explained by the Coulomb energy $e^2/2R$ due to the positive charge appearing on the cluster during the photoemission process. For small clusters, the apparent spin-orbit splitting of the Hg $5d$ levels is smaller than for bulk Hg and even smaller than for isolated Hg atoms. This is attributed to repulsion between the Cd $4d$ and Hg $5d$ orbitals for the smallest clusters, where almost all the Hg atoms are in contact with the $Hg_{1-x}Cd_xTe$ substrate. Finally, we have shown that Hg out-diffusion from the bulk is probably the major reason for the formation of these clusters.

ACKNOWLEDGMENTS

We are grateful to Y. J. Kim for the preparation of some of the samples used for this work. This work carried out at the University of Illinois at Chicago, was supported by the U. S. Defense Advanced Research projects Agency and monitored by the U. S. Air Force Office of Scientific Research under Contract No. F4920-87-C-0021. One of us (R.S.) is supported in part by the Belgian National Foundation for Scientific Research [Fonds National Belge pom la Recherche Scientifique (FNRS)].

*Permanent address: Facultés Universitaires Notre-Dame de la Paix, B-5000 Namur, Belgium.

†Present address: Sandia National Laboratories, Organization 1144, Albuquerque, NM 87185-5800.

[1]K. S. Liang, W. R. Salaneck, and I. A. Aksay, Solid State Commun. **19**, 329 (1976).

[2]M. G. Mason, Phys. Rev. B **27**, 748 (1983).

[3]G. K. Wertheim, S. B. DiCenzo, and S. E. Younquist, Phys. Rev. Lett. **51**, 2310 (1983).

[4]J. C. Slater and K. H. Johnson, Phys. Today **27**, 34 (1974).

[5]T. Kendelewicz, W. G. Petro, I. Lindau, and W. E. Spicer, Phys. Rev. B **30**, 5800 (1984).

[6]F. Houzay, M. Bensoussan, C. Guille, and F. Barthe, Surf. Sci. **162**, 617 (1985).

[7]R. Sporken, P. Xhonneux, R. Caudano, and J. P. Delrue, Surf. Sci. (to be published).

[8]J. Reno, R. Sporken, Y. J. Kim, C. Hsu, and J. P. Faurie, Appl. Phys. Lett. **51**, 1545 (1987).

[9]J. P. Faurie, IEEE J. Quantum Electron. **QE-22**, 1656 (1986).

[10]K. A. Harris, S. Hwang, D. K. Blanks, J. W. Cook, J. F. Schetzina, N. Otsuka, J. B. Baukus, and A. T. Hunter, Appl. Phys. Lett. **48**, 396 (1986).

[11]S. Doniach and M. Šunjić, J. Phys. C **3**, 285 (1970).

[12]C. Hsu, T. M. Duc, and J. P. Faurie (unpublished).

[13]T. Miller, A. P. Shapiro, and T. C. Chiang, Phys. Rev. B **31**, 7915 (1985).

[14]R. Sporken, P. A. Thiry, E. Petit, J. J. Pireaux, R. Caudano, J. Ghijsen, R. L. Johnson, and L. Ley, Phys. Rev. B **35**, 7927 (1987).

[15]G. K. Wertheim, S. B. DiCenzo, and D. N. E. Buchanan, Phys. Rev. B **33**, 5384 (1986).

[16]S. Svensson, N. Martensson, E. Basilier, P. A. Mamquist, U. Gelius, and K. Siegbahn, J. Electron Spectrosc. Relat. Phenom. **9**, 51 (1976).

[17]L. Ley, S. P. Kowalczyk, F. R. McFeely, and D. A. Shirley, Phys. Rev. B **10**, 4881 (1974).
[18]V. L. Moruzzi, A. R. Williams, and J. F. Janak, Phys. Rev. B **10**, 4856 (1974).
[19]W. Eberhardt, S. C. Wu, R. Garrett, D. Sondericker, and F. Jona, Phys. Rev. B **31**, 8285 (1985).
[20]J. P. Faurie, A. Million, R. Roch, and J. L. Tissot, J. Vac. Sci. Technol. A **1**, 1593 (1983); S. Sivananthan, X. Chu, J. Reno, and J. P. Faurie, J. Appl. Phys. **60**, 1359 (1986).